Inorganic Chemistry

FORUM ARTICLE

pubs.acs.org/IC

Oxidation and Reduction of Bis(imino)pyridine Iron Dicarbonyl Complexes

Aaron M. Tondreau,[†] Carsten Milsmann,[†] Emil Lobkovsky,[‡] and Paul J. Chirik*[,†]

[†]Department of Chemistry, Princeton University, Princeton, New Jersey 08540, United States

[‡]Baker Laboratory, Department of Chemistry and Chemical Biology, Cornell University, Ithaca, New York 14853, United States

Supporting Information

ABSTRACT: The oxidation and reduction of a redox-active aryl-substituted bis(imino)pyridine iron dicarbonyl has been explored to determine whether electron-transfer events are ligand- or metal-based or a combination of both. A series of bis(imino)pyridine iron dicarbonyl compounds, $[(^{iPr}PDI)Fe(CO)_2]^-$, $(^{iPr}PDI)Fe(CO)_2$, and $[(^{iPr}PDI)Fe(CO)_2]^+$ [^{iPr}PDI = 2,6-(2,6-$^{i}Pr_2C_6H_3N{=}CMe)_2C_5H_3N$], which differ by three oxidation states, were prepared and the electronic structures evaluated using a combination of spectroscopic techniques and, in two cases, $[(^{iPr}PDI)Fe(CO)_2]^+$ and $[(^{iPr}PDI)Fe(CO)_2]$, metrical parameters from X-ray diffraction. The data establish that the cationic iron dicarbonyl complex is best described as a low-spin iron(I) compound ($S_{Fe} = {}^1/_2$) with a neutral bis(imino)pyridine chelate. The anionic iron dicarbonyl, $[(^{iPr}PDI)Fe(CO)_2]^-$, is also best described as an iron(I) compound but with a two-electron-reduced bis(imino)pyridine. The covalency of the neutral compound, $(^{iPr}PDI)Fe(CO)_2$, suggests that both the oxidative and reductive events are not ligand- or metal-localized but a result of the cooperativity of both entities.

INTRODUCTION

One of the principal challenges in base metal catalysis is to enable two-electron reaction chemistry with transition-metal ions that have kinetically facile and thermodynamically accessible one-electron processes.[1,2] As nature has amply demonstrated in metalloenzymes,[3] radical participation with the surrounding ligands is an effective strategy for overcoming one-electron chemistry to promote a net two-electron transformation. In synthetic compounds, redox-active metal−ligand combinations have emerged as useful platforms to manipulate electronic structure to enable nontraditional redox chemistry[4] and ultimately reactivity[5−8] and catalysis.[4a,9,10]

Bis(imino)pyridine ligands, 2,6-($R^1N{=}CR^2$)$_2C_5H_3N$ (R^1 = alkyl, aryl, amino; R^2 = H, Me), have a long-standing history in classical Werner-type coordination chemistry with first-row transition metals.[11−16] Interest in these ligands was renewed with Brookhart and Gibson's introduction of sterically demanding aryl substituents on the imine and demonstration of their utility in iron- and cobalt-catalyzed ethylene polymerization.[17−20] Our laboratory has since established the catalytic activity of the reduced bis(imino)pyridine iron dinitrogen complex, $(^{iPr}PDI)Fe(N_2)_2$[21] [^{iPr}PDI = 2,6-(2,6-$^{i}Pr_2{-}C_6H_3N{=}CMe)_2$-$C_5H_3N$] in olefin hydrogenation, hydrosilylation, [2 + 2] cycloaddition,[22] and hydrogenative enyne and diyne cyclizations.[23] Significantly improved hydrogenation activity was observed when the size of the 2,6-aryl substituents was reduced to ethyl and methyl groups, e.g., $[(^{R}PDI)Fe]_2(\mu_2\text{-}N_2)_2$ (R = Me, Et).[24]

Spectroscopic and computational studies on compounds with principally σ-donating ligands such as (*N*,*N*-dimethylamino)-pyridine,[25] pyridine, or $^{t}BuNH_2$[26] established that the formal Fe^0 oxidation states are deceiving and that these molecules are best described as intermediate-spin ferrous compounds ($S_{Fe} = 1$) antiferromagnetically coupled to a triplet ($S_{PDI} = 1$) bis(imino)pyridine diradical (Figure 1). These studies expand upon the seminal electrochemical work of Toma and co-workers[27,28] and the preparative and spectroscopic experiments of Wieghardt and co-workers[29,30] that provided the foundation for identifying the redox activity of bis(imino)pyridines[31−34] and implicated the importance of this phenomenon in various reaction types including catalysis[22] and group-transfer chemistry.[35]

The discovery that two-electron reduction is bis(imino)pyridine-based raised the fundamental question of "how many electrons are required to reduce the iron?" in $(^{iPr}PDI)FeL_n$ compounds. It should be noted that Gambarotta and co-workers have reported the ability of the bis(imino)pyridine ligand scaffold to accept up to *three* electrons,[36] rendering assignment of the spectroscopic oxidation states of subsequent reduction products a priori nonobvious. A related question is the oxidation of $(^{iPr}PDI)FeL_n$ compounds; would electron loss be ligand- or metal-based? Here we describe our first efforts toward this objective and report a combined synthetic and spectroscopic effort aimed at understanding the oxidation and reduction of bis(imino)pyridine iron dicarbonyl compounds. These compounds were chosen because the carbonyl ligands were anticipated to be substitutionally inert and offer CO stretching frequencies as an additional diagnostic for probing the electronic structures of the compounds.

RESULTS AND DISCUSSION

Oxidation and Reduction of the Bis(imino)pyridine Iron Dicarbonyl Compound $(^{iPr}PDI)Fe(CO)_2$. The redox chemistry of $(^{iPr}PDI)Fe(CO)_2$ was initially explored electrochemically to

Received: April 8, 2011
Published: June 13, 2011

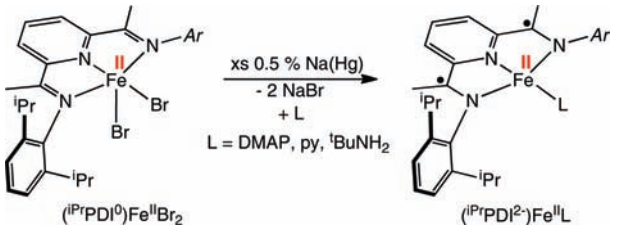

Figure 1. Electronic structures of two-electron-reduced bis(imino)-pyridine iron compounds bearing principally σ-donating ligands.

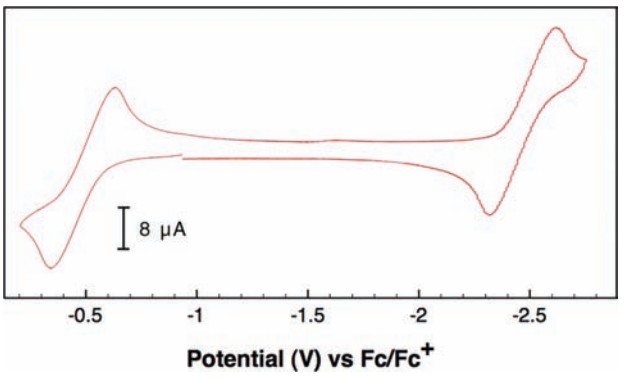

Figure 2. CV of (^{iPr}PDI)Fe(CO)$_2$ (glassy carbon working electrode, 0.1 M [^{n}Bu$_4$N][PF$_6$], scan rate 100 mV/s in THF at 295 K versus ferrocene$^{0/+}$).

determine the chemical accessibility of the oxidized and reduced compounds. Cyclic voltammetry on a 1 mM solution of (^{iPr}PDI)Fe(CO)$_2$ with 0.1 M [^{n}Bu$_4$N][PF$_6$] in a tetrahydrofuran (THF) solution reveals clean and reversible one-electron oxidation and reduction events (Figure 2). Scanning anodically from a starting potential of −0.93 V (vs ferrocene), the cyclic voltammogram (CV) shows an oxidation wave at −0.49 V and a reduction wave at −2.46 V, indicating that both oxidized and reduced bis(imino)pyridine iron carbonyl compounds should be synthetically accessible.

Before the chemical oxidation and reduction chemistry is presented, it is useful to review the electronic structure of the neutral derivative, (^{iPr}PDI)Fe(CO)$_2$. Previous spectroscopic and computational studies from our laboratory[21,25] have established that the ground state for this molecule can be described either as a low-spin iron(II) compound with a singlet (S_{PDI} = 0) dianionic chelate or as a traditional Fe^0 d^8 complex with a neutral bis(imino)pyridine ligand (Figure 3). The reason for the ambiguity derives from the density functional theory (DFT)-computed highest occupied molecular orbital (HOMO) of the compound, which is 68% bis(imino)pyridine in character with a large contribution from the iron center. Unlike (^{iPr}PDI)Fe(N$_2$)$_2$ and other derivatives with weaker field neutral donors,[26] (^{iPr}PDI)Fe(CO)$_2$ exhibits no spectroscopic evidence for the mixing of low-lying higher-spin excited states, and therefore the electronic structure can be considered a hybrid of the Fe^0 and Fe^{II} limiting resonance forms.

The oxidation of (^{iPr}PDI)Fe(CO)$_2$ was initially attempted with [(η^5-C$_5$H$_5$)$_2$Fe][BPh$_4$]. This method proved unsuccessful because the starting bis(imino)pyridine iron dicarbonyl compound was recovered. Use of the ferrocenium reagent with a

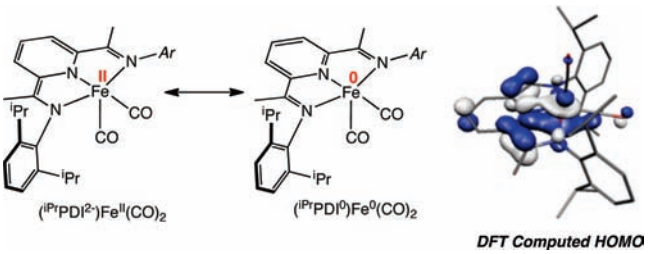

Figure 3. Electronic structure of (^{iPr}PDI)Fe(CO)$_2$ highlighting the hybrid between the (^{iPr}PDI^{2-})Fe^{II}(CO)$_2$ and (^{iPr}PDI^0)Fe^0(CO)$_2$ resonance forms. The DFT-computed HOMO[21,25] is shown to illustrate the covalency in the molecule.

more weakly coordinating anion, [(η^5-C$_5$H$_5$)$_2$Fe][BAr$^F_4$] [BAr$^F_4$ = B(C$_6$H$_3$-3,5-Me$_2$)$_4$], resulted in productive chemistry and furnished a dark-purple-black precipitate identified as the desired cationic bis(imino)pyridine iron dicarbonyl complex, [(^{iPr}PDI)Fe(CO)$_2$][BAr$^F_4$], in 98% yield (eq 1).

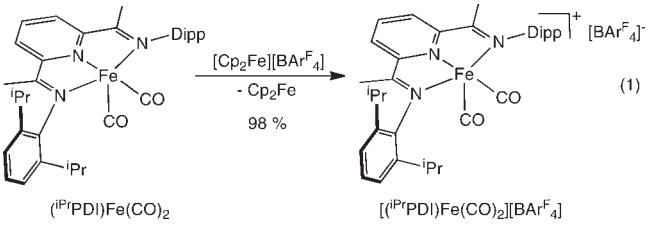

Solid-state magnetic measurements (magnetic susceptibility balance) on [(^{iPr}PDI)Fe(CO)$_2$][BAr$^F_4$] produced an effective magnetic moment of 2.0 μ_B at 290 K, consistent with one unpaired electron and a doublet ground state for the molecule. The poor solubility of the compound in common laboratory solvents such as THF, diethyl ether, and toluene made characterization by ^{1}H NMR spectroscopy challenging. However, dichloromethane-d_2 proved to be a suitable solvent, and the ^{1}H NMR spectrum shows six peaks (out of a possible eight for the C_{2v}-symmetric compound) that are paramagnetically shifted and broadened (see the Experimental Section).

The solid-state (KBr) IR spectrum of [(^{iPr}PDI)Fe(CO)$_2$][BAr$^F_4$] exhibits two strong carbonyl bands at 2028 and 1981 cm^{-1}. These values shift to 1982 and 1937 cm^{-1} upon preparation of the ^{13}C isotopologue, [(^{iPr}PDI)Fe(^{13}CO)$_2$][BAr$^F_4$]. As presented in Table 1, these values are shifted to higher frequency from the neutral analogue and are consistent with the reduced electron density at the iron center, reducing backbonding to the carbonyl ligands.

The solid-state structure of [(^{iPr}PDI)Fe(CO)$_2$][BAr$^F_4$] was determined by X-ray diffraction. Single crystals were obtained from layering of a dichloromethane solution of the compound with diethyl ether. A representation of the molecular structure of the cationic portion of the molecule is presented in Figure 4, while a depiction of the complete ion pair is reported in the Supporting Information. The molecular geometry about the iron center in the cation is best described as idealized square pyramidal, with the bis(imino)pyridine and one carbonyl ligand defining the basal plane. There are no obvious close contacts between the cation and anion.

A comparison of the bond distances for the cationic iron dicarbonyl, [(^{iPr}PDI)Fe(CO)$_2$][BAr$^F_4$], and its neutral analogue, (^{iPr}PDI)Fe(CO)$_2$, is reported in Table 2. The N$_{imine}$−C$_{imine}$

dx.doi.org/10.1021/ic200730k |Inorg. Chem. 2011, 50, 9888–9895

Table 1. Solid-State (KBr) IR Stretching Frequencies for (^{iPr}PDI)Fe(CO)$_2$, [(^{iPr}PDI)Fe(CO)$_2$][BAr$^F_4$], [Na(18-crown-6)(THF)$_2$][(^{iPr}PDI)Fe(CO)$_2$], and ^{13}C Isotopologues (cm^{-1})

compound	ν(CO)$_{sym}$	ν(CO)$_{asym}$
(^{iPr}PDI)Fe(CO)$_2$	1974	1914
(^{iPr}PDI)Fe(^{13}CO)$_2$	1930	1870
[(^{iPr}PDI)Fe(CO)$_2$]$^+$	2028	1981
[(^{iPr}PDI)Fe(^{13}CO)$_2$]$^+$	1982	1937
[(^{iPr}PDI)Fe(CO)$_2$]$^-$	1935	1863
[(^{iPr}PDI)Fe(^{13}CO)$_2$]$^-$	1890	1819

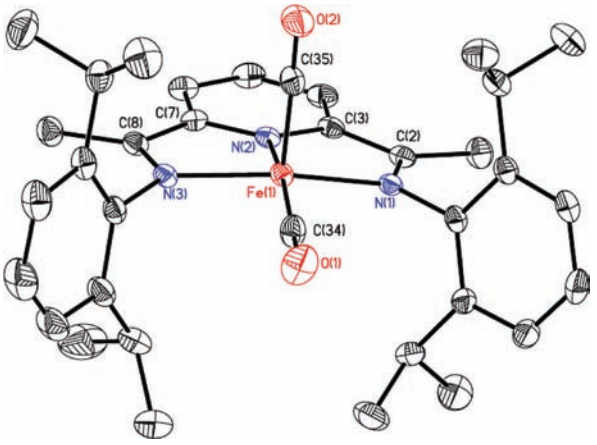

Figure 4. Molecular structure of the cation of [(^{iPr}PDI)Fe(CO)$_2$][BAr$^F_4$] at 30% probability ellipsoids. The anion is omitted for clarity. A representation of the full molecule is presented in the Supporting Information.

Table 2. Selected Bond Distances (Å) and Angles (deg) for [(^{iPr}PDI)Fe(CO)$_2$][BAr$^F_4$] and (^{iPr}PDI)Fe(CO)$_2$[a]

	[(^{iPr}PDI)Fe(CO)$_2$][BAr$^F_4$]	(^{iPr}PDI)Fe(CO)$_2$
Fe(1)−N(1)	1.984(4)	1.9500(14)
Fe(1)−N(2)	1.877(2)	1.8488(14)
Fe(1)−N(3)	1.985(4)	1.9622(15)
Fe(1)−C(34)	1.801(4)	1.7823(19)
Fe(1)−C(35)	1.811(4)	1.7809(19)
N(1)−C(2)	1.289(4)	1.335(2)
N(3)−C(8)	1.289(4)	1.330(2)
N(2)−C(3)	1.348(4)	1.376(2)
N(2)−C(7)	1.350(4)	1.372(2)
C(2)−C(3)	1.462(4)	1.423(2)
C(7)−C(8)	1.459(4)	1.425(2)
C(34)−O(1)	1.124(4)	1.147(2)
C(35)−O(2)	1.128(4)	1.148(2)
N(1)−Fe(1)−N(2)	79.49(10)	79.10(6)
N(1)−Fe(1)−N(3)	154.39(10)	152.56(6)
N(2)−Fe(1)−N(3)	78.99(10)	79.32(6)
N(2)−Fe(1)−C(34)	167.36(14)	157.89(8)
N(2)−Fe(1)−C(35)	98.51(13)	105.09(8)
C(34)−Fe(1)−C(35)	94.13(16)	97.01(9)

[a] The values for (^{iPr}PDI)Fe(CO)$_2$ were taken from ref 21.

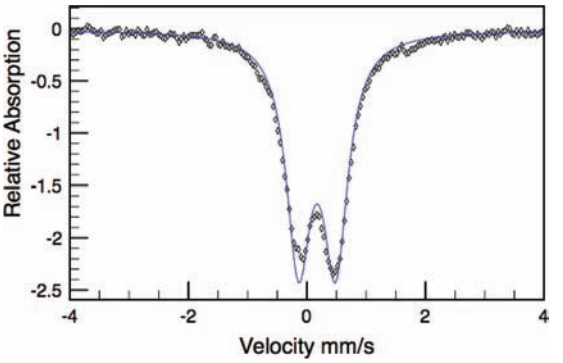

Figure 5. Zero-field ^{57}Fe Mössbauer spectrum of [(^{iPr}PDI)Fe(CO)$_2$][BAr$^F_4$] recorded at 80 K.

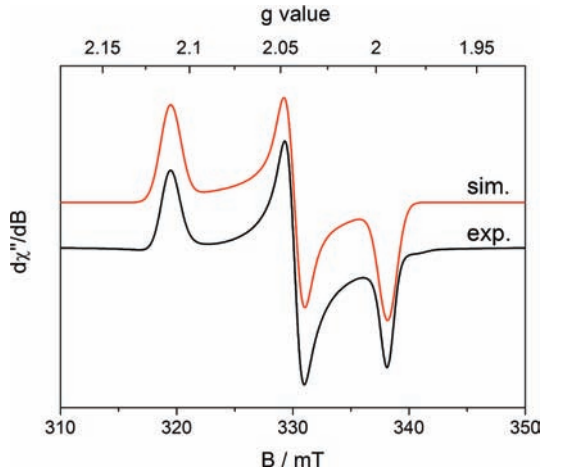

Figure 6. X-band EPR spectrum of [(^{iPr}PDI)Fe(CO)$_2$][BAr$^F_4$] recorded at 4.2 K in 1:1 toluene:dichloromethane glass.

bond distances of 1.289(4) and 1.289(4) Å, and the C$_{ipso}$−C$_{imine}$ lengths of 1.462(4) and 1.459(4) Å in the cation establish that the bis(imino)pyridine ligand is in its neutral form. By contrast, the bis(imino)pyridine distances in the neutral iron dicarbonyl, (^{iPr}PDI)Fe(CO)$_2$, exhibit significant perturbation consistent with contributions from a closed-shell, dianionic form of the chelate. In combination with the magnetic data, the observation of a neutral, redox-innocent chelate in the cation, [(^{iPr}PDI)Fe(CO)$_2$][BAr$^F_4$], suggests a low-spin iron(I) compound.

The electronic structure of [(^{iPr}PDI)Fe(CO)$_2$][BAr$^F_4$] was also studied by zero-field Mössbauer spectroscopy. A representative spectrum is presented in Figure 5. An isomer shift (δ) of 0.17 mm/s and a quadrupole splitting (ΔE_Q) of 0.62 mm/s were measured. The value of δ increases from 0.03 mm/s upon oxidation of the neutral compound, (^{iPr}PDI)Fe(CO)$_2$, while the quadrupole splitting decreases from 1.17 mm/s. The changes in both the isomer shift and quadrupole splitting are consistent with oxidation of a highly covalent Fe^{II} ↔ Fe^0 compound to a more metal-centered radical, low-spin, iron(I) derivative.

The X-band electron paramagnetic resonance (EPR) spectrum of [(^{iPr}PDI)Fe(CO)$_2$][BAr$^F_4$] was recorded in a 1:1 dichloromethane/toluene glass at 4.2 K. The experimental spectrum and its simulation are presented in Figure 6. A rhombic signal is observed, and the fit of the data yielded the following g values: g_{min} = 1.994, g_{mid} = 2.043, and g_{max} = 2.111, consistent

dx.doi.org/10.1021/ic200730k |Inorg. Chem. 2011, 50, 9888–9895

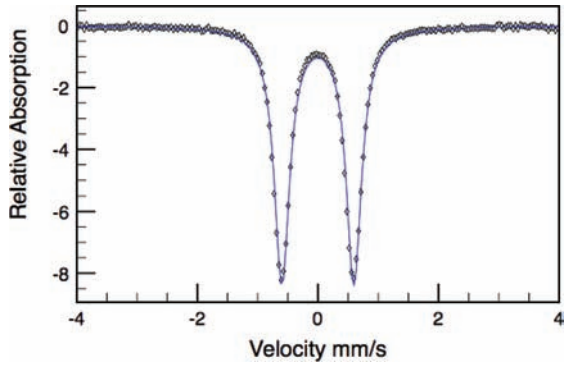

Figure 7. Zero-field ^{57}Fe Mössbauer spectrum of [Na-15-crown-5][(^{iPr}PDI)Fe(CO)$_2$] recorded at 80 K.

with an $S = {}^1/_2$ compound. The g anisotropy indicates an iron- rather than ligand-based radical as the singly occupied molecalur orbital (SOMO) of the compound. The spectrum of the ^{13}CO isotopologue, [(^{iPr}PDI)Fe(^{13}CO)$_2$][BAr$^F{}_4$], recorded under the same conditions did not exhibit any detectable differences from the natural abundance compound.

The one-electron reduction of (^{iPr}PDI)Fe(CO)$_2$ proved more challenging than the corresponding oxidation, consistent with the electrochemistry (Figure 2). Stirring (^{iPr}PDI)Fe(CO)$_2$ in the presence of excess 0.5% Na(Hg) did not yield an identifiable compound. Considerable amounts of the starting neutral iron dicarbonyl compound were recovered. Repeating the reduction procedure with excess 0.5% Na(Hg) in the presence of 1.2 equiv of 15-crown-5 furnished a green precipitate. Analysis of the product mixture by solid-state (KBr) IR spectroscopy revealed *six* bands; the largest two appear at 1935 and 1863 cm^{-1} and are assigned to the desired iron dicarbonyl dianion, [Na-15-crown-5][(^{iPr}PDI)Fe(CO)$_2$] (eq 2). These values are at lower energy than the neutral and cationic variants, consistent with a more electron-rich iron center. The four other CO bands observed in the spectrum are attributed to unidentified decomposition products.

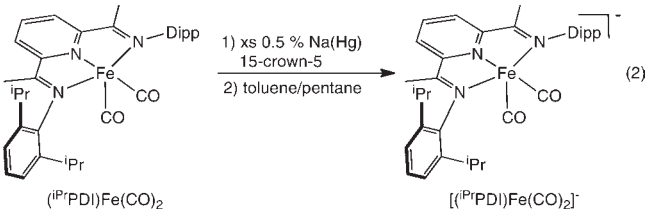

Obtaining [Na-15-crown-5][(^{iPr}PDI)Fe(CO)$_2$] in pure form was challenging because the molecule proved highly sensitive and prone to decomposition. The compound was only sparingly soluble in toluene, THF, and diethyl ether. Chlorinated solvents such as dichloromethane induced immediate decomposition. For solvents where partial solubility was observed, decomposition occurred over the course of approximately 24 h. In the solid state, [Na-15-crown-5][(^{iPr}PDI)Fe(CO)$_2$] was stable for weeks if stored in an inert atmosphere at −35 °C. To obtain clean spectroscopic data on [Na-15-crown-5][(^{iPr}PDI)Fe(CO)$_2$], the green solid isolated from the reduction reaction was washed with copious amounts of toluene, followed by pentane, and the resulting materials were quickly dried under reduced pressure. Unfortunately, attempts to obtain single crystals of this compound have thus far been unsuccessful.

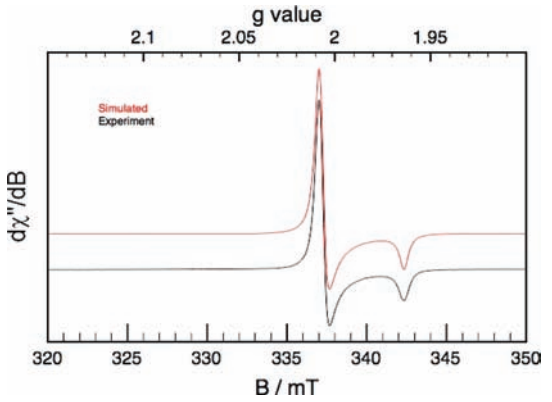

Figure 8. X-band EPR spectrum of [Na-15-crown-5][(^{iPr}PDI)Fe(CO)$_2$] recorded at 77 K in toluene glass.

The electronic structure of [Na-15-crown-5][(^{iPr}PDI)Fe(CO)$_2$] was also explored by zero-field ^{57}Fe Mössbauer (Figure 7) and EPR (Figure 8) spectroscopies. The Mössbauer parameters (δ = −0.01 mm/s; ΔE_Q = 1.19 mm/s) for the anion are indistinguishable from those of the neutral complex (δ = 0.03, ΔE_Q = 1.19 mm/s), suggesting little perturbation to the electronic environment of the iron nucleus upon reduction. The X-band EPR spectrum, recorded in toluene glass at 77 K, exhibits an axial signal consistent with an $S = {}^1/_2$ compound. Values obtained from the fit are g_{min} = 1.974, g_{mid} = 2.004, and g_{max} = 2.006. The g anisotropy (Δg = 0.032) is low and suggests a ligand-based rather than an iron-based SOMO.

Computational Studies. The electronic structures of the bis(imino)pyridine iron dicarbonyl cation and anion were examined by DFT. Our laboratory has demonstrated the utility of augmenting experimentally obtained structural and spectroscopic data with DFT calculations to fully understand the electronic structure of redox-active bis(imino)pyridine iron compounds.[25,37] Complete spectroscopic and computational determination of the electron structure of the neutral compound, (^{iPr}PDI)Fe(CO)$_2$, has been reported previously.[25] Broken-symmetry (BS) DFT calculations were performed at the B3LYP level to understand the electronic structures of [(^{iPr}PDI)Fe(CO)$_2$]$^+$ and [(^{iPr}PDI)Fe(CO)$_2$]$^-$. For both the cation and anion, the corresponding counterions [BAr$^F{}_4$]$^-$ and [Na-15-crown-5]$^+$ were not included in the calculations, respectively. No other truncations were performed.

The cationic bis(imino)pyridine iron dicarbonyl compound, [(^{iPr}PDI)Fe(CO)$_2$]$^+$, was computed as a spin-unrestricted doublet, in agreement with the experimentally established ground state. The resulting ground state did not exhibit any significant BS character, as is nicely shown by the expectation value of $\hat{S}^2$ of 0.76 (ideally 0.75 for $S = {}^1/_2$). The computed structural parameters of the molecule obtained after geometry optimization are in excellent agreement with the experimentally observed values. A qualitative molecular orbital diagram and Mulliken spin density plot from the ground-state solution are presented in Figure 9. From these studies, [(^{iPr}PDI)Fe(CO)$_2$]$^+$ is best described as a low-spin iron(I) compound with three doubly occupied principally iron-based d orbitals and a SOMO that is primarily Fe d_{z^2} in character. As illustrated by both the molecular orbital diagram and the spin density plot, the bis(imino)pyridine ligand is in its neutral form with little direct involvement in the overall electronic structure of the complex.

dx.doi.org/10.1021/ic200730k |*Inorg. Chem.* 2011, 50, 9888–9895

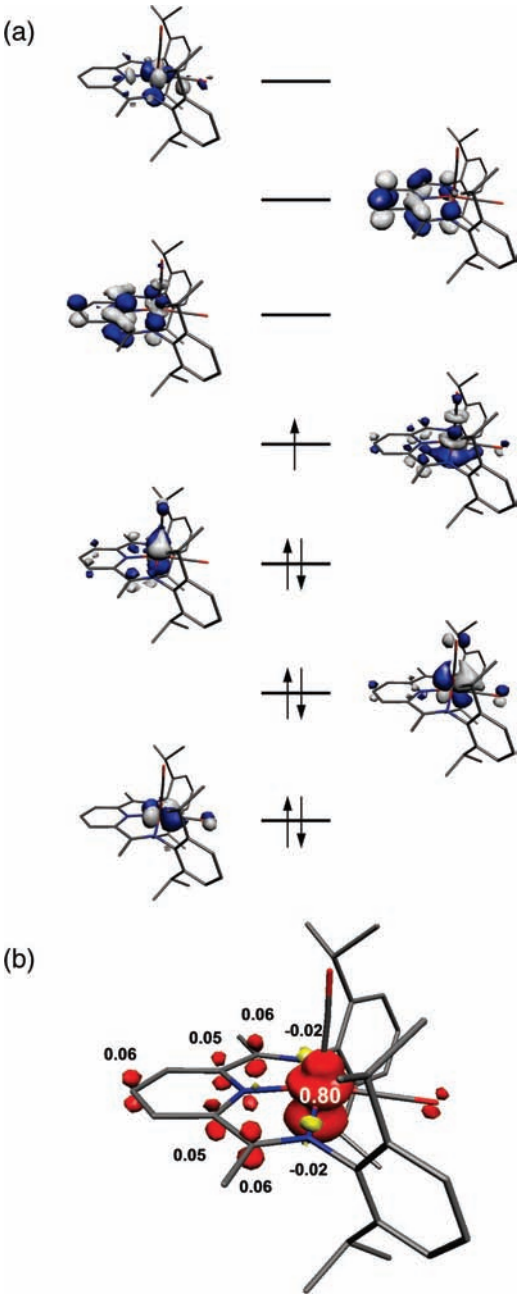

Figure 9. (a) Qualitative molecular orbital diagram for $[(^{iPr}PDI)Fe(CO)_2]^+$ from a spin-unrestricted B3LYP DFT calculation. (b) Spin density plot obtained from a Mulliken population analysis (red, positive spin density; yellow, negative spin density). The coordinate axis is defined as the z direction, being the apical vector of an idealized square pyramid.

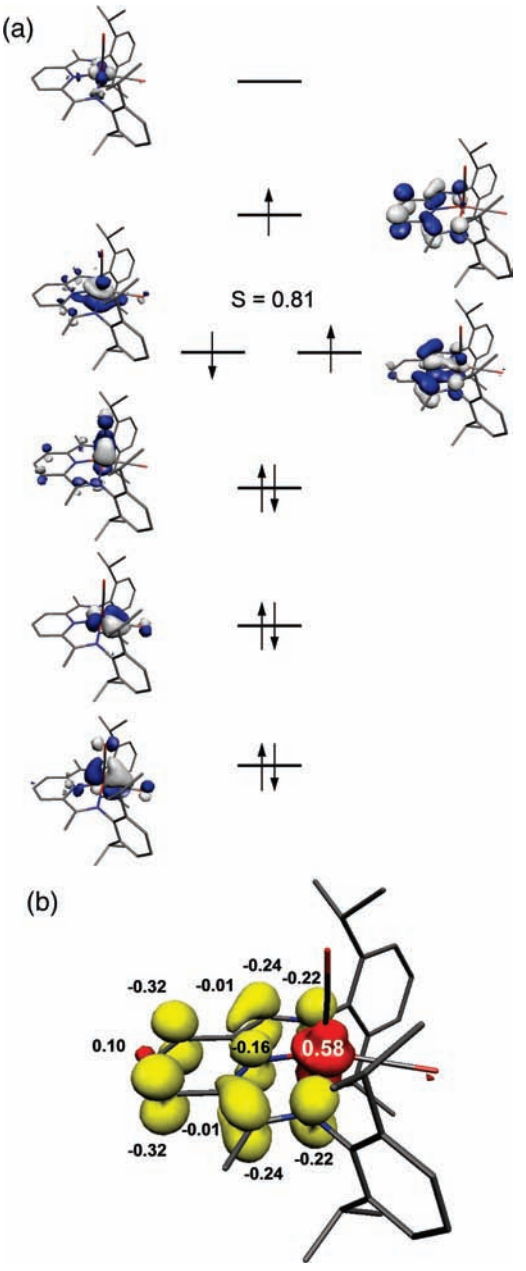

Figure 10. (a) Qualitative molecular orbital diagram for $[(^{iPr}PDI)Fe(CO)_2]^-$ from a spin-unrestricted B3LYP DFT calculation. S represents the spatial overlap of the antiferromagnetically coupled magnetic orbitals. (b) Spin density plot obtained from a Mulliken population analysis (red, positive spin density; yellow, negative spin density). The coordinate axis is defined as the z direction, being the apical vector of an idealized square pyramid.

This view of the electronic structure is in agreement with the metrical parameters established from X-ray diffraction and the dichloromethane glass EPR spectrum of the compound. To further support the validity of the calculated electronic structure, ^{57}Fe Mössbauer parameters were computed. The obtained isomer shift of 0.24 mm/s and the quadrupole splitting of −0.85 mm/s are in good agreement with the experimentally determined values.

The computational results for the bis(imino)pyridine iron dicarbonyl anion, $[(^{iPr}PDI)Fe(CO)_2]^-$, are presented in Figure 10. The geometry-optimized structure (Table S1 in the Supporting Information) is consistent with a strongly reduced bis(imino)-pyridine ligand with long $N_{imine}-C_{imine}$ bond distances of 1.362 Å and short $C_{ipso}-C_{imine}$ bonds of 1.414 Å. Accordingly, the ground state arises from a BS (2,1) solution ($\hat{S}^2$ = 1.11),[38] with the electronic structure of the molecule best described as a low-spin iron(I) compound with a triplet (S_{PDI} = 1) bis(imino)pyridine diradical. Antiferromagnetic coupling between the iron and bis-(imino)pyridine ligand spins accounts for the overall $S = {}^1/_2$ ground state. It should be noted that the value of S of 0.81, a measure of the

dx.doi.org/10.1021/ic200730k |*Inorg. Chem.* 2011, 50, 9888–9895

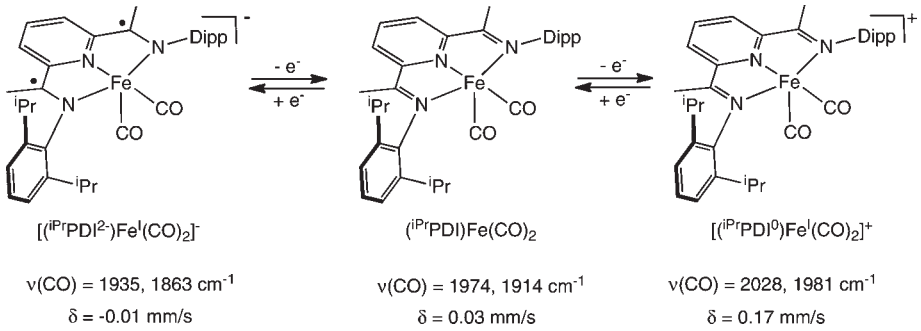

Figure 11. Electronic structure summary for bis(imino)pyridine iron dicarbonyl compounds that differ by three oxidation states.

spatial overlap between magnetic orbitals, is large. This indicates a high degree of covalency in the molecule and suggests that the true electronic structure is more complex than the relatively simple $[(^{iPr}PDI^{2-})Fe^{I}(CO)_2]^{-}$ assignment. Nevertheless, the computational results clearly establish a doubly reduced bis(imino)pyridine chelate and shed additional light on the electronic structure of $[(^{iPr}PDI^{2-})Fe^{I}(CO)_2]^{-}$ because the instability of the molecule has hampered structural characterization. This is also reflected in the correct prediction of the Mössbauer spectrum based on the electronic structure described above. The computed parameters of δ = 0.08 mm/s and ΔE_Q = −1.39 mm/s are in reasonable agreement with the experimental values.

A summary of the spectroscopic data and electronic structures for the series of bis(imino)pyridine iron dicarbonyl compounds is presented in Figure 11. Each of the electronic structures presented in Figure 11 has been corroborated by DFT calculations. The most oxidized compound in the series, $[(^{iPr}PDI)Fe(CO)_2]^{+}$, is a rare example of a spectroscopically characterized bis(imino)pyridine iron(I) compound. Interestingly, if the neutral iron dicarbonyl, $[(^{iPr}PDI)Fe(CO)_2]$, is viewed in its low-spin ferrous canonical form, the overall oxidation of the molecule results in a net reduction of the iron. A formal two-electron loss from the chelate triggers a reduction of the iron from Fe^{II} to Fe^{I}. This phenomenon has been observed previously with redox-active bis(imino)pyridine metal complexes.[29]

The most reduced compound in the series, the bis(imino)pyridine iron dicarbonyl anion, $[(^{iPr}PDI)Fe(CO)_2]^{-}$, is best described as a low-spin iron(I) compound with a triplet bis(imino)pyridine diradical dianion. The DFT studies established a high degree of covalency in the molecule, consistent with the observed low Mössbauer isomer shift, and suggest that the $[(^{iPr}PDI^{2-})Fe^{I}(CO)_2]^{-}$ description is likely an oversimplification. Nevertheless, the DFT results clearly establish a diradical form of the chelate, the only compound in the series to exhibit radical character on the ligand.

EXPERIMENTAL SECTION

General Considerations. All air- and moisture-sensitive manipulations were carried out using standard vacuum-line, Schlenk-line, and cannula techniques in an MBraun inert-atmosphere drybox containing an atmosphere of purified nitrogen. Solvents for air- and moisture-sensitive manipulations were initially dried and deoxygenated using literature procedures.[39] Benzene-d_6 was purchased from Cambridge Isotope Laboratories and dried over 4 Å molecular sieves. The neutral bis(imino)pyridine iron dicarbonyl compound, $(^{iPr}PDI)Fe(CO)_2$, was prepared according to literature methods.[21] The ^{13}C isotopologue, $(^{iPr}PDI)Fe(^{13}CO)_2$, was synthesized in an identical manner using ^{13}CO.

^{1}H NMR spectra were recorded on Varian Mercury 300 and Inova 400, 500, and 600 spectrometers operating at 299.76, 399.78, 500.62, and 599.78 MHz, respectively. ^{13}C NMR spectra were recorded on an Inova 500 spectrometer operating at 125.893 MHz. All ^{1}H and ^{13}C NMR chemical shifts are reported relative to $SiMe_4$ using the ^{1}H (residual) and ^{13}C chemical shifts of the solvent as a secondary standard. Peak widths at half heights are reported for paramagnetically broadened and shifted resonances. Solution magnetic moments were determined by the Evans method using a ferrocene standard and are the average value of at least two independent measurements. Gouy balance measurements were performed with a Johnson Matthey instrument that was calibrated with $HgCo(SCN)_4$. Elemental analyses were performed at Robertson Microlit Laboratories, Inc., in Madison, NJ.

Single crystals suitable for X-ray diffraction were coated with polyisobutylene oil in a drybox, transferred to a nylon loop, and then quickly transferred to the goniometer head of a Bruker X8 APEX2 diffractometer equipped with a molybdenum X-ray tube (λ = 0.710 73 Å). Preliminary data revealed the crystal system. A hemisphere routine was used for data collection and determination of lattice constants. The space group was identified, and the data were processed using the Bruker *SAINT+* program and corrected for absorption using *SADABS*. The structures were solved using direct methods (*SHELXS*) completed by subsequent Fourier synthesis and refined by full-matrix least-squares procedures.

Mössbauer data were collected on an alternating constant-acceleration spectrometer. The minimum experimental line width was 0.24 mm/s (full width at half-height). A constant sample temperature was maintained with an Oxford Instruments Variox or an Oxford Instruments Mössbauer-Spectromag 2000 cryostat. Reported isomer shifts (δ) are referenced to iron metal at 293 K. CVs were collected in a THF solution [1 mM in $(^{iPr}PDI)Fe(CO)_2$] with 0.1 M $[^{n}Bu_4N][PF_6]$ (0.1 M) electrolyte, using a 3 mm glassy carbon working electrode, platinum wire as the counter electrode, and silver wire as the reference electrode in a drybox equipped with electrochemical outlets. CVs were recorded using a BASi EC Epsilon electrochemical workstation and analyzed using the BASi Epsilon-EC software. All CVs were run at a scan rate of 100 mV/s at 295 K. Potentials are reported versus ferrocence/ferrocenium and were obtained using the in situ method.[40]

Quantum-Chemical Calculations. All DFT calculations were performed with the *ORCA* program package.[41] The geometry optimizations of the complexes and single-point calculations on the optimized geometries were carried out at the B3LYP level[42−44] of DFT. This hybrid functional often gives better results for transition-metal compounds than pure gradient-corrected functionals, especially with regard to metal−ligand covalency.[45] The all-electron Gaussian basis sets were those developed by Ahlrichs' group.[46−48] Triple-ζ quality basis sets def2-TZVP with one set of polarization functions on the metals and on the atoms directly coordinated to the metal center were used. For the carbon and

dx.doi.org/10.1021/ic200730k |*Inorg. Chem.* 2011, 50, 9888–9895

hydrogen atoms, slightly smaller polarized split-valence def2-SV(P) basis sets were used that were of double-ζ quality in the valence region and contained a polarizing set of d functions on the non-hydrogen atoms. Auxiliary basis sets were chosen to match the orbital basis.[49−51] The RIJCOSX[52−54] approximation was used to accelerate the calculations.

Throughout this paper we describe our computational results by using the BS approach by Ginsberg[55] and Noodleman et al.[56] Because several BS solutions to the spin-unrestricted Kohn−Sham equations may be obtained, the general notation BS(m,n)[57] has been adopted, where m (n) denotes the number of spin-up (spin-down) electrons at the two interacting fragments. Canonical and corresponding[58] orbitals, as well as spin density plots, were generated with the program *Molekel*.[59]

Nonrelativistic single-point calculations on the optimized geometry were carried out to predict Mössbauer spectral parameters (isomer shifts and quadrupole splittings). These calculations employed the CP(PPP) basis set for iron.[60] The Mössbauer isomer shifts were calculated from the computed electron densities at the iron centers as previously described.[61,62]

Preparation of [(^{iPr}PDI)Fe(CO)$_2$][BArF$_{24}$]. A 20 mL scintillation vial was charged with 0.110 g (0.185 mmol) of (^{iPr}PDI)Fe(CO)$_2$, 0.200 g (0.184 mmol) of [Cp$_2$Fe][BArF$_{24}$], and a stir bar. With stirring, approximately 7 mL of benzene was added to the mixture of solids. The rate of stirring was increased as the reaction mixture thickened and a precipitate formed. After 15 min, an equal volume of pentane was added, and the stirring was continued for an additional 10 min. The resulting solid was collected on a glass frit and washed four times with ∼20 mL of pentane. The solid was dried in vacuo and yielded 0.260 g (98%) of a dark-black-purple powder identified as [(^{iPr}PDI)FeCO$_2$][BArF$_{24}$]. Elem anal. Calcd for $C_{67}H_{55}N_3FeBF_{24}O_2$: C, 55.24; H, 3.81; N, 2.88. Found: C, 55.33; H, 3.67; N, 2.81. IR (KBr): ν(CO) 2028 and 1981, ν(^{13}CO) 1982 and 1937 cm^{-1}. Solid-state magnetic susceptibility (23 °C): μ_{eff} = 2.0 μ_B. ^{1}H NMR (dichloromethane-d_2): δ 1.40 (569 Hz), 4.32 (370 Hz), 7.35 (18 Hz), 7.58 (12 Hz), 7.76 (15 Hz), 9.44 (45 Hz).

Preparation of [Na(15-crown-5)][(^{iPr}PDI)Fe(CO)$_2$]. A 20 mL scintillation vial was charged with 0.200 g (0.337 mmol) of (^{iPr}PDI)Fe(CO)$_2$ and 10 mL of diethyl ether. A 1% sodium amalgam (6 equivalents) was prepared in a separate vial in pentane. The amalgam was added to the stirring iron solution. After the amalgam was added, 0.080 g (1.1 equiv) of 15-crown-5 was added. The resulting solution was stirred for approximately 60 min, during which time a bright-green precipitate formed and was collected on a glass frit. The green powder was washed three times with ∼10 mL of toluene and pentane to yield 0.120 g (43%) of a green powder identified as [Na-15-crown-5][(^{iPr}PDI)Fe(CO)$_2$]. Elem anal. Calcd for $C_{45}H_{63}FeN_3NaO_7$: C, 64.59; H, 7.59; N, 5.02. Found: C, 64.50; H, 7.58; N, 4.64. IR (KBr): ν(CO) 1935 and 1863, ν(^{13}CO) 1890 and 1819 cm^{-1}. Solid-state magnetic susceptibility (23 °C): μ_{eff} = 1.9 μ_B.

■ ASSOCIATED CONTENT

Supporting Information. Crystallographic details for [(^{iPr}PDI)Fe(CO)$_2$][BAr$^F{}_4$] in CIF format and DFT-computed bond distances. This material is available free of charge via the Internet at http://pubs.acs.org.

■ AUTHOR INFORMATION

Corresponding Author
*E-mail: pchirik@princeton.edu.

■ ACKNOWLEDGMENT

We thank the U.S. National Science Foundation and Deutsche Forschungsgemeinschaft for a Cooperative Activities in Chemistry between U.S. and German Investigators grant. We also thank Jon Darmon and Dr. Suzanne Bart for performing the electrochemical studies.

■ REFERENCES

(1) Chirik, P. J.; Wieghardt, K. *Science* **2010**, *327*, 5967.
(2) Dzik, W. I.; van der Vlugt, J.; Reek, J. N. H.; De Bruin, B. *Angew. Chem.* **2011**, *50*, 3356.
(3) (a) Kaim, W.; Scwederski, B. *Coord. Chem. Rev.* **2010**, *254*, 1580. (b) Meunier, B.; de Visser, S. P.; Shaik, S. *Chem. Rev.* **2004**, *104*, 3947. (c) Whittaker, J. W. *Chem. Rev.* **2003**, *103*, 2347. (d) Jazdzewski, B. A.; Tolman, W. B. *Coord. Chem. Rev.* **2000**, *200−202*, 633. (e) Stubbe, J.; Van der Donk, W. A. *Chem. Rev.* **1998**, *98*, 706.
(4) (a) Nguyen, A. I.; Zarkesh, R. A.; Lacy, D. C.; Thorson, M. K.; Heyduk, A. F. *Chem. Sci.* **2011**, *2*, 166. (b) Nguyen, A. I.; Blackmore, K. J.; Carter, S. M.; Zarkesh, R. A.; Heyduk, A. F. *J. Am. Chem. Soc.* **2009**, *131*, 3307. (c) Blackmore, K. J.; Sly, M. B.; Haneline, M. R.; Ziller, J. W.; Heyduk, A. F. *Inorg. Chem.* **2008**, *47*, 10522. (d) Blackmore, K. J.; Ziller, J. W.; Heyduk, A. F. *Inorg. Chem.* **2005**, *44*, 5559.
(5) Stanciu, C.; Jones, M. E.; Fanwick, P. E.; Abu-Omar, M. M. *J. Am. Chem. Soc.* **2007**, *129*, 12400.
(6) Lippert, C. A.; Arnstein, S. A.; Sherrill, C. D.; Soper, J. D. *J. Am. Chem. Soc.* **2010**, *132*, 3879.
(7) King, E. R.; Betley, T. A. *Inorg. Chem.* **2009**, *48*, 2361.
(8) Puschmann, F. F.; Harner, J.; Stein, D.; Ruegger, H.; de Bruin, B.; Grützmacher, H. *Angew. Chem., Int. Ed.* **2010**, *49*, 385.
(9) Smith, A. L.; Hardcastle, K. I.; Soper, J. D. *J. Am. Chem. Soc.* **2010**, *132*, 14358.
(10) Dzik, W. I.; Xu, X.; Zhang, X. P.; Reek, J. N. H.; de Bruin, B. *J. Am. Chem. Soc.* **2010**, *132*, 10891.
(11) Figgins, P. E.; Busch, D. H. *J. Am. Chem. Soc.* **1960**, *82*, 820.
(12) Stouffer, R. C.; Hadley, W. B.; Busch, D. H. *J. Am. Chem. Soc.* **1961**, *83*, 3732.
(13) Schmidt, J. G.; Brey, W. S.; Stoufer, R. C. *Inorg. Chem.* **1967**, *6*, 268.
(14) Curry, J. D.; Robinson, M. A.; Busch, D. H. *Inorg. Chem.* **1967**, *6*, 1570.
(15) Sacconi, L.; Morassi, R.; Midollini, S. *J. Chem. Soc. A* **1968**, 1510.
(16) Davis, R. N.; Tanski, J. M.; Adrian, J. C.; Tyler, L. A. *Inorg. Chim. Acta* **2007**, *360*, 3061.
(17) Bianchini, C.; Giambastiani, G.; Rios, I. G.; Mantovani, G.; Meli, A.; Segarra, A. M. *Coord. Chem. Rev.* **2006**, *250*, 1391.
(18) Britovsek, G. J. P.; Gibson, V. C.; Kimberley, B. S.; Maddox, S. J.; Solan, G. A.; White, A. J. P.; Williams, D. J. *Chem. Commun.* **1998**, 849.
(19) (a) Small, B. M.; Brookhart, M. *J. Am. Chem. Soc.* **1998**, *120*, 7143. (b) Small, B. L.; Brookhart, M.; Bennett, A. M. A. *J. Am. Chem. Soc.* **1998**, *120*, 4049.
(20) Britovsek, G. J. P.; Bruce, M.; Gibson, V. C.; Kimberely, B. S.; Maddox, P. J.; Mastroianni, S.; McTavish, S. J.; Redshaw, C.; Solan, G. A.; Strömberg, S.; White, A. J. P.; Williams, D. J. *J. Am. Chem. Soc.* **1999**, *121*, 8728.
(21) Bart, S. C.; Lobkovsky, E.; Chirik, P. J. *J. Am. Chem. Soc.* **2004**, *126*, 13794.
(22) Bouwkamp, M. W.; Bowman, A. C.; Lobkovsky, E.; Chirik, P. J. *J. Am. Chem. Soc.* **2006**, *128*, 13340.
(23) Sylvester, K. T.; Chirik, P. J. *J. Am. Chem. Soc.* **2009**, *131*, 8772.
(24) Russell, S. K.; Darmon, J. M.; Lobkovsky, E.; Chirik, P. J. *Inorg. Chem.* **2010**, *49*, 2782.
(25) Bart, S. C.; Chlopek, K.; Bill, E.; Bouwkamp, M. W.; Lobkovsky, E.; Neese, F.; Wieghardt, K.; Chirik, P. J. *J. Am. Chem. Soc.* **2006**, *128*, 13901.
(26) Bart, S. C.; Lobkovsky, E.; Bill, E.; Wieghardt, K.; Chirik, P. J. *Inorg. Chem.* **2007**, *46*, 7055.
(27) Kuwabara, I. H.; Comninos, F. C. M.; Pardini, V. L.; Viertler, H.; Toma, H. E. *Electrochim. Acta* **1994**, *39*, 2401.

(28) Toma, H. E.; Chavez-Gil, T. E. *Inorg. Chim. Acta* **1997**, *257*, 197.
(29) de Bruin, B.; Bill, E.; Bothe, E.; Weyermüller, T.; Wieghardt, K. *Inorg. Chem.* **2000**, *39*, 2936.
(30) Budzelaar, P. H. M.; de Bruin, B.; Gal, A. W.; Wieghardt, K.; van Lenthe, J. H. *Inorg. Chem.* **2001**, *40*, 4649.
(31) Chaudhuri, P.; Wieghardt, K. *Prog. Inorg. Chem.* **2001**, *50*, 151.
(32) (a) Knijnenburg, Q.; Gambarotta, S.; Budzelaar, P. H. M. *Dalton Trans.* **2006**, 5442. (b) Bart, S. C.; Chlopek, K.; Bill, E.; Bouwkamp, M. W.; Lobkovsky, E.; Neese, F.; Wieghardt, K.; Chirik, P. J. *J. Am. Chem. Soc.* **2006**, *128*, 13901.
(33) Butin, K. P.; Beloglazkina, E. K.; Zyk, N. V. *Russ. Chem. Rev.* **2005**, *74*, 531.
(34) Wile, B. M.; Trovitch, R. J.; Bart, S. C.; Tondreau, A. M.; Lobkovsky, E.; Milsmann, C.; Bill, E.; Wieghardt, K.; Chirik, P. J. *Inorg. Chem.* **2009**, *48*, 4190.
(35) Bart, S. C.; Lobkovsky, E.; Bill, E.; Chirik, P. J. *J. Am. Chem. Soc.* **2006**, *128*, 5302.
(36) Enright, D.; Gambarotta, S.; Yap, G. P. A.; Budzelaar, P. H. M. *Angew. Chem., Int. Ed.* **2002**, *41*, 3873.
(37) Bowman, A. C.; Milsmann, C.; Bill, E.; Lobkovsky, E.; Weyermüller, T.; Wieghardt, K.; Chirik, P. J. *Inorg. Chem.* **2010**, *49*, 6110.
(38) The BS(*m*,*n*) descriptor refers to a broken-symmetry state with *m* unpaired spin-up electrons on fragment 1 and *n* spin-down electrons on fragment 2.
(39) Pangborn, A. B.; Giardello, M. A.; Grubbs, R. H.; Rosen, R. K.; Timmers, F. J. *Organometallics* **1996**, *15*, 1518.
(40) Geiger, W. E. *Organometallics* **2007**, *26*, 5738.
(41) Neese, F. *ORCA: an ab initio, DFT and Semiempirical Electronic Structure Package*, version 2.8, revision 2287; Institut für Physikalische und Theoretische Chemie, Universität Bonn: Bonn, Germany, Nov 2010.
(42) Becke, A. D. *J. Chem. Phys.* **1986**, *84*, 4524.
(43) Becke, A. D. *J. Chem. Phys.* **1993**, *98*, 5648.
(44) Lee, C. T.; Yang, W. T.; Parr, R. G. *Phys. Rev. B* **1988**, *37*, 785.
(45) Neese, F.; Solomon, E. I. In *Magnetism: From Molecules to Materials*; Miller, J. S., Drillon, M., Eds.; Wiley: New York, 2002; Vol. 4, p 345.
(46) Schäfer, A.; Horn, H.; Ahlrichs, R. *J. Chem. Phys.* **1992**, *97*, 2571.
(47) Schäfer, A.; Huber, C.; Ahlrichs, R. *J. Chem. Phys.* **1994**, *100*, 5829.
(48) Weigend, F.; Ahlrichs, R. *Phys. Chem. Chem. Phys.* **2005**, *7*, 3297.
(49) Eichkorn, K.; Weigend, F.; Treutler, O.; Ahlrichs, R. *Theor. Chem. Acc.* **1997**, *97*, 119.
(50) Eichkorn, K.; Treutler, O.; Öhm, H.; Häser, M.; Ahlrichs, R. *Chem. Phys. Lett.* **1995**, *240*, 283.
(51) Eichkorn, K.; Treutler, O.; Öhm, H.; Häser, M.; Ahlrichs, R. *Chem. Phys. Lett.* **1995**, *242*, 652.
(52) Neese, F.; Wennmohs, F.; Hansen, A.; Becker, U. *Chem. Phys.* **2009**, *356*, 98.
(53) Kossmann, S.; Neese, F. *Chem. Phys. Lett.* **2009**, *481*, 240.
(54) Neese, F. *J. Comput. Chem.* **2003**, *24*, 1740.
(55) Ginsberg, A. P. *J. Am. Chem. Soc.* **1980**, *102*, 111.
(56) Noodleman, L.; Peng, C. Y.; Case, D. A.; Mouesca, J. M. *Coord. Chem. Rev.* **1995**, *144*, 199.
(57) Kirchner, B.; Wennmohs, F.; Ye, S.; Neese, F. *Curr. Opin. Chem. Biol.* **2007**, *11*, 134.
(58) Neese, F. *J. Phys. Chem. Solids* **2004**, *65*, 781.
(59) *Molekel*, Advanced Interactive 3D-Graphics for Molecular Sciences, available under http://www.cscs.ch/molkel/.
(60) Neese, F. *Inorg. Chim. Acta* **2002**, *337*, 181.
(61) Sinnecker, S.; Slep, L. D.; Bill, E.; Neese, F. *Inorg. Chem.* **2005**, *44*, 2245.
(62) Römelt, M.; Ye, S.; Neese, F. *Inorg. Chem.* **2009**, *48*, 784.